Geophysical Research Letters

RESEARCH LETTER
10.1029/2020GL091588

Exceptionally Persistent Madden-Julian Oscillation Activity Contributes to the Extreme 2020 East Asian Summer Monsoon Rainfall

Wenjun Zhang[1], Zongci Huang[1], Feng Jiang[1], Malte F. Stuecker[2], Guosen Chen[1], and Fei-Fei Jin[3]

[1]CIC-FEMD/ILCEC, Key Laboratory of Meteorological Disaster of Ministry of Education (KLME), Nanjing University of Information Science and Technology, Nanjing, China, [2]Department of Oceanography & International Pacific Research Center (IPRC), School of Ocean and Earth Science and Technology, University of Hawai'i at Mānoa, Honolulu, HI, USA, [3]Department of Atmospheric Sciences, School of Ocean and Earth Science and Technology, University of Hawai'i at Mānoa, Honolulu, HI, USA

Key Points:

- The rainfall amount over the East Asian plum-rain belt during summer 2020 was the largest in the recent four decades
- The intense flooding coincided with an exceptionally persistent Madden-Julian Oscillation (MJO) active phase in the Indian Ocean throughout June and July
- This extraordinary MJO activity was facilitated by the conducive pantropic background oceanic-atmospheric conditions

Supporting Information:

- Supporting Information S1

Correspondence to:
W. Zhang,
zhangwj@nuist.edu.cn

Citation:
Zhang, W., Huang, Z., Jiang, F., Stuecker, M. F., Chen, G., & Jin, F.-F. (2021). Exceptionally persistent Madden-Julian Oscillation activity contributes to the extreme 2020 East Asian summer monsoon rainfall. *Geophysical Research Letters*, *48*, e2020GL091588. https://doi.org/10.1029/2020GL091588

Received 5 NOV 2020
Accepted 11 FEB 2021

Abstract During June–July 2020, the record-breaking flooding in the recent four decades struck the plum rain belt over China, Japan, and Korea. Concurrent with this persistent heavy rainfall, pronounced Indian Ocean basin warming (IOBW) was observed, following the previous El Niño event in the transition to La Niña-like mean state this summer. This tropical Indo-Pacific large-scale thermal condition provided favorable conditions for rainfall surpluses over the plum rain belt via the western North Pacific anticyclone. Superimposed on the tropical Indo-Pacific large-scale thermal condition, an extraordinary long-lasting and quasistationary Madden-Julian Oscillation (MJO) active phase persisted in the Indian Ocean throughout June–July 2020, lasting for 59 days. The MJO-associated teleconnection was mainly responsible for the extreme rainfall over the plum rain belt, which was facilitated by the conducive large-scale Indo-Pacific oceanic-atmospheric condition.

Plain Language Summary The East Asian rainy season (commonly called the plum rain, also known as Meiyu in China, Baiu in Japan, and Jangma in Korea), is caused by rainfall along a persistent stationary front. The plum rain season usually starts in June and persists into the middle of July. During June–July 2020, the region of the plum rain belt over China, Japan, and Korea, was ravaged by the strongest flooding in decades with catastrophic losses. The physical mechanisms driving this extreme flooding remains unclear. Concurrent with this persistent rainfall surpluses, the Indo-Pacific oceans featured a developing La Niña-like state in the eastern tropical Pacific and pronounced sea surface temperature warming in the Indian Ocean basin. Although these Indo-Pacific thermal conditions can provide a favorable large-scale background for the rainfall surpluses over East Asia, they cannot explain the extreme rainfall amount over the plum rain belt during 2020. We show that an exceptionally long-lasting and quasistationary Madden-Julian Oscillation activity over the Indian Ocean was the key reason for this extreme event.

1. Introduction

The plum rain (Meiyu in China, Baiu in Japan, and Jangma/Changma in Korea) extending from middle China to southern Japan through Korea during boreal summer (June–July), usually accounts for about 30%–40% of the annual total rainfall there (e.g., T. J. G. Chen & Chang, 1980; Ninomiya & Shibagaki, 2007; Tao & Chen, 1987). It exhibits pronounced interannual variability and is usually characterized by large rainfall deficiencies and surpluses accompanied by huge economic losses (e.g., Ding et al., 2007; Ninomiya & Shibagaki, 2007; Sampe & Xie, 2010; B.Wang & Lin, 2002). During summer 2020, the region of the plum rain belt over China, Japan, and Korea suffered devastating rainfall extremes, which was the largest on record in the recent four decades (Figure 1). Investigations on the possible mechanisms explaining these exceptional floods are of tremendous importance for the potential future predictability of similar extreme climate events, allowing for disaster prevention and mitigation.

Concurrent with the extreme plum rainfall, prominent sea surface temperature (SST) anomalies were evident over the tropical Indian and Pacific Oceans. The structure of the tropical Pacific SST anomalies seems

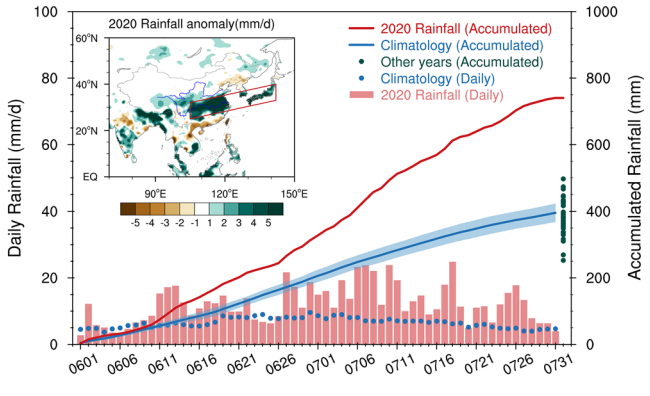

Figure 1. Daily rainfall (bar; mm/d; left *y*-axis) and daily accumulated rainfall (red line; mm; right *y*-axis) over the plum rain belt (red box in the inset) from June 1 to July 31 of 2020. Blue dots and the blue line indicate climatological daily rainfall (mm/d, left *y*-axis) and climatological daily accumulated rainfall (mm, right *y*-axis), respectively. The blue shading denotes one standard deviation of the accumulated rainfall. The green dots represent the accumulated rainfall (mm; right *y* axis) in all other years (from 1980 to 2019). The inset shows rainfall anomalies (shading; mm/d) during June–July 2020.

to be associated with an El Niño transition to a La Niña-like (with far eastern tropical Pacific cooling while not being identified as a La Niña event yet) state. Coincide with the El Niño-Southern Oscillation (ENSO) phase transition, a remarkable Indian Ocean basin warming (IOBW) can be detected over the Indian Ocean (IO), analogous to the conventional IO SST response to El Niño events. The IOBW, the dominant mode of the IO SST variability, commences its development in boreal winter, peaks in spring, and persists into summer, which typically lags the El Niño peak phase by about one season (e.g., Alexander et al., 2002; Klein et al., 1999; Li et al., 2003; Xie et al., 2016; J. Yang et al., 2007).

El Niño decaying summers usually witness an anomalous low-level anticyclone over the western North Pacific (WNP) (e.g., Stuecker et al., 2015; B. Wang et al., 2000; Zhang et al., 1999). This anomalous anticyclone is initiated and maintained by the interaction of ENSO with the warm pool seasonal cycle (e.g., Stuecker et al., 2013, 2015; W. Zhang et al., 2015, 2016) or by the WNP local air-sea interaction via the wind-evaporation-SST feedback (B. Wang et al., 2000). In addition, the remote IOBW can also exert significant impacts on the anomalous WNP anticyclone as an Indian Ocean (IO) capacitor effect (Xie et al., 2016; J. Yang et al., 2007). The anomalous WNP anticyclone leads to an enhanced moisture influx from the tropical oceans toward East Asia, thereby causing rainfall surpluses. It seems that the June–July 2020 Indo-Pacific SST conditions could provide a preferred large-scale thermal background for the rainfall surpluses over East Asia.

Superimposed on these SST conditions, an extraordinary strong and stationary Madden-Julian Oscillation (MJO; Madden & Julian, 1971) activity was detected in the IO during June–July 2020. The typical MJO is the dominant component of the intraseasonal (30–90 days) variability in the tropical atmosphere, manifesting itself in a slow eastward propagation of deep convection coupled with the atmospheric circulation (e.g., Zhang, 2005). Previous studies show that the MJO activities have an influence on the summer rainfall over Southeast China in intraseasonal time scales, which tends to increase when the MJO convection mainly locates over the IO and to decrease while the MJO enters the western Pacific (e.g., L. Zhang et al., 2009). In contrast to traditional MJO events, the MJO-associated convection in summer 2020 unexpectedly stalled in the western IO throughout June and July. It is compelling to hypothesize that this sustained active MJO phase in the IO may have contributed to the extreme rainfall over the plum rain belt.

However, the underlying mechanisms driving the extreme climate event in June–July 2020 remain unclear. Here, we use reanalysis products and statistical analyses to investigate the physical forcing responsible for the extreme climate event over the plum rain belt.

2. Data and Methodology

Global monthly SST anomalies are investigated based on the National Oceanic and Atmospheric Administration (NOAA) Extended Reconstructed SST analysis, version 5 (ERSSTv5, Huang et al., 2017) with a horizontal resolution of 2° × 2°. The utilized rainfall data include the Climate Prediction Center (CPC) Unified Gauge-Based Analysis of Daily Precipitation data set at 0.5° horizontal resolution (P. Xie et al., 2007) and monthly mean data of CPC Merged Analysis of Precipitation (P. Xie & Arkin, 1997) at 2.5° horizontal resolution. The monthly and daily mean atmospheric reanalysis on a 2.5° × 2.5° grid is obtained from the National Centers for the Environmental Prediction-Department of Energy (NCEP-DOE) Atmospheric Model Intercomparison Project-II data set (Kanamitsu et al., 2002). The daily mean outgoing longwave radiation (OLR) data provided by NOAA from http://www.esrl.noaa.gov/psd/are also used. Our analyses cover the period from 1980 to 2020 and anomalies are derived relative to the monthly mean climatology (1980–2020). The plum rain season (June–July) is our focus in this study. To focus on the intraseasonal variability when analyzing the impact of the MJO on the rainfall over the plum rain belt, the annual cycle (mean and first

three harmonics of climatological annual variation) is removed from the daily mean OLR and 850-hPa zonal wind, and the running mean of the previous 120 days is also subtracted to exclude the effects of inter-annual variability (Lee et al., 2013; Wheeler & Hendon, 2004). All statistical significance tests are performed based on the two-tailed Student's *t*-test.

ENSO events are defined according to the CPC's definition based on a threshold of ±0.5°C of the Niño3.4 index (averaged SST anomaly in the domain of 5°S-5°N, 120°W-170°W) for five consecutive months. We identify 12 El Niño events (1982/1983, 1987/1988, 1991/1992, 1994/1995, 1997/1998, 2002/2003, 2004/2005, 2006/2007, 2009/2010, 2015/2016, 2018/2019, 2019/2020),14 La Niña events (1983/1984, 1984/1985, 1988/1989, 1995/1996, 1998/1999, 1999/2000, 2000/2001, 2005/2006, 2007/2008, 2008/2009, 2010/2011, 2011/2012, 2016/2017, 2017/2018) and eight El Niño to La Niña transition summers (1983, 1988, 1995, 1998, 2005, 2007, 2010, 2016). We examine the sensitivity of the consecutive La Niña events on the composite results by removing these events or only considering the first year, and qualitative conclusions remain the same. The IOBW index is defined as the area-averaged SST anomalies over the tropical IO (20°S-20°N, 40°E-110°E) following a previous study (J. Yang et al., 2007). The daily real-time multivariate MJO (RMM) indices (RMM1 and RMM2) (Wheeler & Hendon, 2004) are available from the Australian Bureau of Meteorology (http://www.bom.gov.au/climate/mjo/). An active MJO day is defined when the MJO amplitude (represented by $(RMM1^2+RMM2^2)^{1/2}$) exceeds one standard deviation.

3. Results

Figure 1 displays the spatial and temporal structures of the plum rain during June–July 2020. Remarkable rainfall surpluses are seen over the middle-lower reaches of the Yangtze River in China, Korea, and southern Japan (the plum rain belt marked as the red box) with maximum rainfall anomalies reaching as high as 5 mm/d. The daily rainfall (red bar) over the plum rain belt exceeded the climatology (blue dot) for the majority of days (52 out of 61 days). Especially, more than 30% days received strong rainfall surpluses, defined by being twice as large as the climatology. The extreme character of the rainfall in June–July 2020 is clearly displayed by the daily accumulated rainfall (red line). From the middle of June to the end of July, the rainfall accumulation in 2020 was far beyond one standard deviation over the plum rain belt (blue shading), being the wettest plum rain season since 1980. The accumulated rainfall in June–July 2020 reached up to 700 mm, much higher than the second highest value (~500 mm) of 1980.

Concurrent with this extremely persistent rainfall over the plum rain belt, pronounced SST anomalies were evident in the tropical Indo-Pacific Oceans, characterized by a developing La Niña-like state in the tropical Pacific and IOBW in June–July 2020 (Figure 2a). The SST cooling in the far eastern tropical Pacific did not meet the ENSO cold phase criterion in this season, however, it would develop into a La Niña state in the ensuing winter. This developing La Niña condition was preceded by a moderate El Niño event according to the CPC's definition, indicating that the summer 2020 was a transition phase from an El Niño to La Niña-like state. To detect El Niño's impacts during its decaying summer phase, we regressed the June–July 850-hPa wind and rainfall anomalies on the preceding winter Niño3.4 index (Figure 2b). A dipole structure in rainfall anomalies was observed over the Indo-Pacific warm pool and a corresponding anomalous anticyclone was evident in the WNP during the El Niño decaying June–July, consistent with the previous studies (e.g., B. Wang et al., 2000; Zhang et al., 1999). The anomalous anticyclone tends to transport more tropical moisture into East Asia and enhance the rainfall there. However, weak rainfall anomalies are shown in part of the plum rain belt, mainly over the Yangtze River (Figure 2b). No statistically significant relationship ($r = 0.21$, insignificant at the 95% confidence level) is detected between the preceding winter Niño3.4 index and June–July rainfall anomalies over the plum rain belt (Figure 3a). We also show regressed 850-hPa wind and rainfall anomalies onto the June–July Niño3.4 index to examine the simultaneous impacts of the La Niña-like condition. The rainfall and wind anomaly patterns over the tropics are very different from those during 2020 and correspondingly no evident rainfall anomalies are observed over the East Asian plum rain belt (Figure S1). Altogether, it seems that the ENSO associated Pacific SST anomalies had minor direct impacts on the rainfall over the plum rain belt during summer 2020.

As mentioned in Section 1, El Niño events tend to produce IOBW during and after its mature phase, which further exerts impacts on the WNP atmospheric circulation and associated rainfall over East Asia during

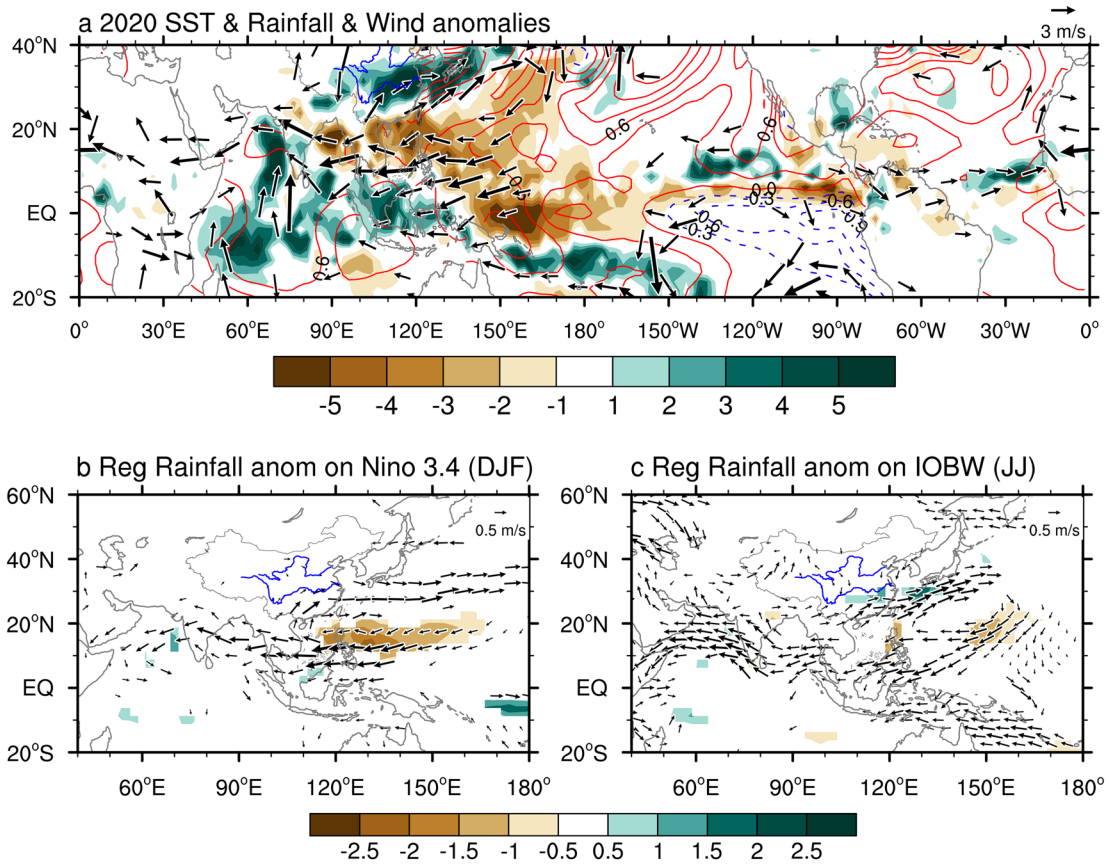

Figure 2. (a) SST (contours; value interval: 0.3°C; red and blue for positive and negative values, respectively) and rainfall anomalies (shading; mm/d), superimposed by the 850 hPa wind anomalies (vectors; m/s; only showing values exceeding 2 m/s) during June–July 2020. Regressed June–July rainfall (shading; mm/d; only showing values that are statistically significant at the 95% confidence level) and 850 hPa wind anomalies (vectors; m/s; only showing values that are statistically significant at the 95% confidence level) onto (b) the preceding winter (December-January-February) Niño3.4 index and (c) the simultaneous IOBW indices.

summer (Xie et al., 2016; J. Yang et al., 2007). To inspect the IOBW-associated climate impacts, we show in Figure 2c the regressed atmospheric circulation and rainfall anomaly patterns. The IOBW coincides with an anomalous anticyclone covering the WNP and northeastern IO, and rainfall surpluses over the plum rain belt. Therefore, we hypothesize that the IO SST condition provided a preferred large-scale background state for enhanced rainfall over the plum rain belt. It is further supported by a linear relationship ($r = 0.44$, significant at the 95% confidence level) between the IOBW and rainfall anomalies over the plum rain belt (Figure 3b).

However, whether these large-scale conditions were a driver for the extreme rainfall in summer 2020 needs to be answered, considering the minor role of the Pacific SST (Figure 3a) and the fact that the IOBW condition in 2020 does not follow the linear relationship shown in Figure 3b. The relatively ineffective role of the Pacific SST anomalies on the plum rain was supported by the absence of the local air-sea coupling in summer 2020 (Figure 3c), which suggests as a key pathway for tropical Pacific thermal conditions to impact the East Asian climate. In the equatorial Pacific, the suppressed convection associated with La Niña events usually occur over the west edge of the SST cooling at around 150°E. During June–July 2020, the negative rainfall anomalies over the western Pacific were located away from the far eastern Pacific cooling. Unexpectedly, they were observed in the region with warm SST anomalies (Figure 3c). It suggests that the suppressed rainfall could not be triggered by either the far eastern Pacific SST cooling or the local SST warming. These SST anomalies in the tropical Pacific were unlikely to play an active role in the extreme rainfall over the plum rain belt. To further examine the IO air-sea condition related to the IOBW, we here reconstruct the 2020 June–July rainfall anomalies over the tropical IO based on the IOBW index and compare it with

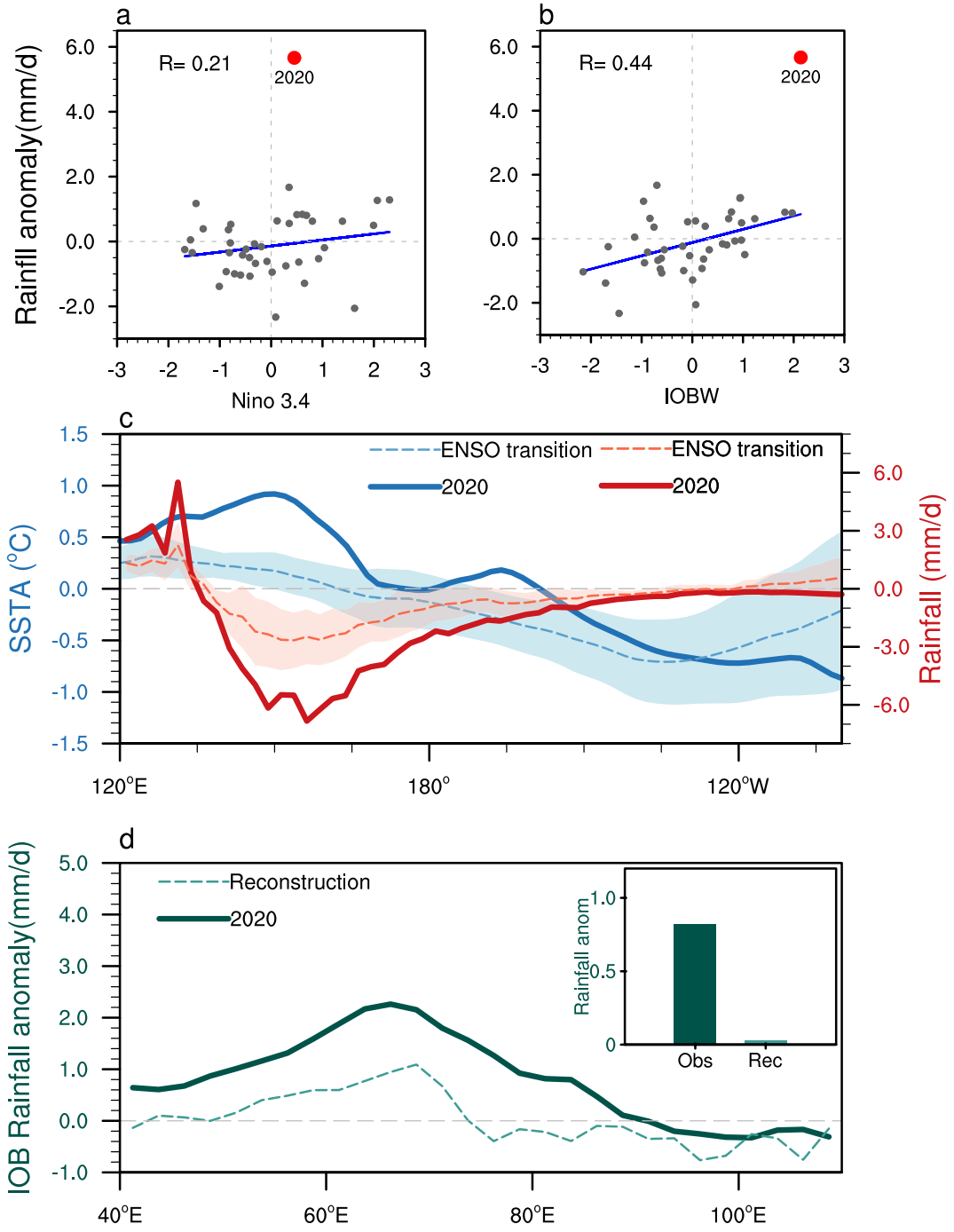

Figure 3. (a) Scatterplot between the preceding winter Niño3.4 index and June–July rainfall anomaly over the plum rain belt ($R = 0.21$ without including the year 2020 that is marked as the red dot). (b) Same as (a), but for the scatterplot between the simultaneous IOBW index and rainfall anomaly ($R = 0.44$ without including the year 2020 that is marked as the red dot). (c) June–July averaged SST (thick blue line; °C; left *y*-axis) and rainfall anomaly (thick red line; mm/d; right *y*-axis) distributions along the equator (2°S-2°N average) in 2020. For comparison, the composited SST (thin blue line; °C; left *y*-axis) and rainfall anomalies (thin red line; mm/d; right *y*-axis) with corresponding one standard deviation (shading) are displayed for the ENSO transition (El Niño to La Niña) summers (June–July), respectively. (d) The June–July averaged rainfall anomaly (mm/d) distribution along the tropical Indian Ocean (20°S-20°N average) in 2020 (solid green line) and the corresponding reconstruction based on the IOBW index (dashed green line). The inset shows the observed (dark green bar) and reconstructed (light green bar) IO (40°E-110°E, 20°S-20°N) rainfall anomalies.

the observations (Figure 3d). The observed rainfall is enhanced over the entire IO Basin with a maximum anomaly around 2.5 mm/day around 70°E (solid line), while the reconstruction shows much weaker positive rainfall anomalies over the western IO and even negative anomalies over the eastern IO (dashed line). The discrepancy can be more clearly shown by IO (40°E-110°E, 20°S-20°N) averaged rainfall anomalies (bar). The reconstruction is much weaker than the observations, suggesting that the IOBW cannot well explain the local convection anomalies and therefore the extreme rainfall in June–July 2020.

Superimposed on the large-scale SST warming in the IO, an exceptionally persistent quasistationary MJO activity was observed during June–July 2020, very different from the eastward-propagating features seen typically for MJO events. Tropical MJO-associated convection activity has been long recognized as an important factor contributing to extreme temperature and rainfall anomalies over East Asia (e.g., Y. Chen & Zhai, 2017; Hong & Li, 2009; Hsu et al., 2020). During 2020, the MJO remained in Phases 1–3 (the tropical IO) throughout June–July with 59 active days during these 2 months (Figure 4a), far beyond the climatology (Figure 4c). To investigate the possible linkage of this unusual MJO event with the East Asian climate, we in Figures 4b and S2 composite the OLR and 850-hPa wind anomalies of the active days in these three phases during early summer 2020 and other years, respectively (Note that the qualitative results with MJO phases 1–2 only remain the same). Corresponding to the enhanced convection in the IO, an anomalous anticyclonic circulation and suppressed convection prevail over the WNP, which brings abundant moisture from the tropical Indo-Pacific oceans to East Asia (Figure S2a). Similar atmospheric circulation and convection anomalies occurred during June–July 2020 (Figure 4b). The most striking feature that distinguishes the year 2020 from other years is the long-lasting active convection in the IO (Figure 4c). The active days (59 days) in Phases 1–3 during June–July 2020 were near 4 times as many as the climatological mean (16 days). This persistent quasistationary MJO convection activity in the IO and its associated WNP anticyclonic anomalies provided a continuous supply of tropical moisture for the long-lasting rainfall over the plum rain belt. Note that about 65% of these active days experienced a very strong MJO activity with an amplitude exceeding 1.5 standard deviation (Figure S3), which led to much stronger intensity during 2020 than composition of other years (Figure 4b).

We next show the time evolution of rainfall anomalies over the plum rain belt (Figure 4d) to highlight the importance of the MJO on the extreme plum rain in 2020. Weakly positive rainfall anomalies occurred during February–March. Then, the rainfall was slightly reduced in April and returned to normal in May. In June–July, the plum rain suddenly increased with averaged anomalies near 6 mm/d. In conjunction with the rainfall evolution, the IOBW maintained within 0.4°C–0.6°C throughout the first half of 2020, which seems not sufficient to account for the sudden rainfall increase in June–July. This increase of the rainfall coincided with a rapid change of the MJO active days in Phases 1–3 (Figure 4d). These results again support that the exceptionally persistent MJO was a main driver for the extreme plum rain in June–July 2020. It is noted that in April 2020, there were 18 MJO active days in Phases 1–3, however, only weakly negative rainfall anomalies were observed over the plum rain belt, consistent with the composite rainfall in previous years (Figure S4). Thus, it seems that the MJO in Phases 1–3 has less effect on rainfall over the plum rain belt during April, suggesting that the MJO impacts on the East Asian rainfall are strongly modulated by the seasonal cycle.

4. Discussion

The MJO during summer (June–July) 2020 exhibited very different propagation features from traditional MJO events, with strong activities maintaining in the IO (Phases 1–3) for up to 59 days. The active MJO in the IO produced an anomalous low-level anticyclone over the WNP that brought continuously abundant moisture to East Asia from the tropical oceans. Therefore, the exceptionally long-lasting MJO activity in June–July 2020 contributed to the extreme rainfall over the plum rain belt under a conducive background state (i.e., the positive IOBW). The abnormal MJO activity needs to be considered in the mechanisms driving regional extreme climate events, which hints to potential predictability of future similar events.

Not coincidentally, many extreme climate events in recent years can be linked to similar abnormal MJO activities with relatively longer phase duration (i.e., slower propagation). For instance, the southeastern Asian floods during 2011 coincided with prolonged MJO activity over the Maritime Continent (MC) and the west

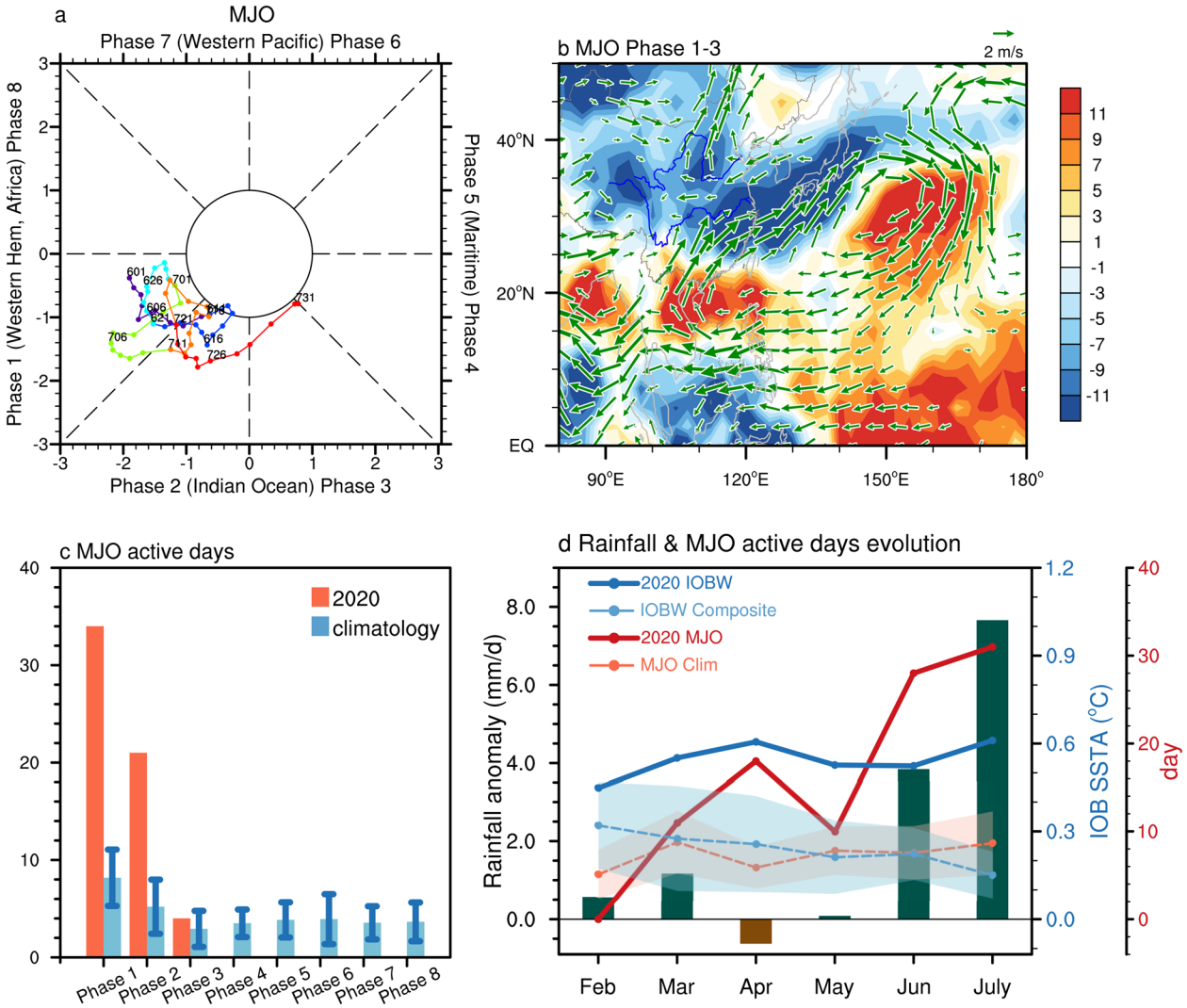

Figure 4. (a) The phase space diagram of MJO from June 1 to July 31, 2020. Each color represents 10 days from June 1st to July 31st and the numbers correspond to the date. (b) Composite OLR (shading; W/m^2) and 850 hPa wind anomalies (green vectors; m/s; only showing values that are statistically significant at the 95% confidence level) of active MJO days in Phases 1–3 during June–July 2020. (c) MJO active days in Phases 1–8 during June–July 2020 (red bar; day) and the climatological mean (blue bar; day) with corresponding one standard deviation (error bars). The active days are selected when the MJO amplitude $(RMM1^2+RMM2^2)^{1/2}$ exceeds 1. (d) Time evolutions of the rainfall anomaly (bar; mm/d; left *y*-axis) over the plum rain belt, the active days staying in MJO Phases 1–3 (thick red line; day; right *y*-axis) and the IOBW index (thick blue line; °C; right *y*-axis) from February to July 2020. For comparison, the climatological mean active days staying in MJO Phases 1–3 (thin red line; day; right *y*-axis) and the composite IOBW index for other El Niño decaying years (thin blue line; °C; right *y*-axis) with corresponding one standard deviation (shading) are displayed.

Pacific (Phases 5–7) (Roxy et al., 2019). Despite several potential theories for MJO propagation so far (e.g., Adames & Kim, 2016; G. Chen & Wang, 2020; Emanuel, 1987; Lau & Peng, 1987; Majda & Stechmann, 2009; B. Wang et al., 2016; L. Wang et al., 2018; D. Yang & Ingersoll, 2013), the underlying mechanism for these irregular quasistationary MJO events remains elusive. A comparison with other similar MJO active years (Figure S5) may provide some possible perspectives for understanding the unusual nature of the June–July 2020 MJO activity. Here, we define years with strong and long-lasting MJO activity during June–July when the MJO active days in Phases 1–3 exceeded 25 days (It is noted that the results remain the same when we chose 30 days or 20 days as the threshold). In these analog years, there is pronounced warming in the tropical western and central IO as well as western Pacific (Figure S6a). This strengthened SST gradient between the Indo-Pacific warm pool and eastern Pacific and associated anomalous easterly winds in the lower troposphere could be one reason for adverse conditions for the MJO propagation over the MC and western Pacific (e.g., Maloney, 2009; Sobel et al., 2014; Zhao et al., 2013). Additionally, the strengthened vertical

easterly shear (defined as the background zonal wind difference between easterly anomalies at 850 hPa and westerly anomalies at 200 hPa) also hinders an eastward propagation of MJO (Lu & Hsu, 2017; C. Zhang & Dong, 2004). In June–July 2020, the SST, lower tropospheric wind, and vertical easterly shear anomalies were all similar to the composite for other MJO active years but with much stronger amplitude (Figures S6b and S6c). We hypothesize that these strongly adverse factors contributed to the MJO activity staying in the central-western IO throughout June–July 2020. These potential controlling mechanisms deserve further attention in the future to improve our understanding of the dynamics of quasistationary MJO events. In the future warming world, the intensity and frequency of extreme climate events are projected to increase (e.g., Min et al., 2011; Zhao et al., 2010). The background warming may contribute to this extreme event, which also deserves further investigation.

Data Availability Statement

The data used to reproduce the results of this paper are located at https://psl.noaa.gov/data/gridded/data.noaa.ersst.v5.html, https://psl.noaa.gov/data/gridded/data.ncep.reanalysis2.pressure.html, https://psl.noaa.gov/data/gridded/data.cpc.globalprecip.html, https://psl.noaa.gov/data/gridded/data.cmap.html, https://psl.noaa.gov/data/gridded/data.interp_OLR.html, and https://psl.noaa.gov/data/gridded/data.uninterp_OLR.html.

Acknowledgments
This work was supported by the National Key Research and Development Program (2018YFC1506002) and the National Nature Science Foundation of China (42088101). This is SOEST publication 11275 and IPRC contribution 1505.

References

Adames, Á. F., & Kim, D. (2016). The MJO as a dispersive, convectively coupled moisture wave: Theory and observations. *Journal of the Atmospheric Sciences*, *73*, 913–941. https://doi.org/10.1175/JAS-D-15-0170.1

Alexander, M. A., Bladé, I., Newman, M., Lanzante, J. R., Lau, N. C., & Scott, J. D. (2002). The atmospheric bridge: The influence of ENSO teleconnections on air–sea interaction over the global oceans. *Journal of Climate*, *15*, 2205–2231.

Chen, G., & Wang, B. (2020). Circulation factors determining the propagation speed of the Madden-Julian Oscillation. *Journal of Climate*, *33*, 3367–3380.

Chen, T. J. G., & Chang, C.-P. (1980). The structure and vorticity budget of an early summer monsoon trough (Mei-Yu) over southeastern China and Japan. *Monthly Weather Review*, *108*, 942–953.

Chen, Y., & Zhai, P. (2017). Simultaneous modulations of precipitation and temperature extremes in southern parts of China by the boreal summer intraseasonal oscillation. *Climate Dynamics*, *49*(9–10), 3363–3381. https://doi.org/10.1007/s00382-016-3518-4

Ding, Y. H., Liu, J. J., Sun, Y., Liu, Y. J., He, J. H., & Song, Y. F. (2007). A study of the synoptic-climatology of the Meiyu system in East Asia. *Chinese Journal of the Atmospheric Sciences*, *31*(6), 1082–1101 (in Chinese).

Emanuel, K. A. (1987). An air–sea interaction model of intraseasonal oscillations in the tropics. *Journal of the Atmospheric Sciences*, *44*, 2324–2340.

Hong, C.-C., & Li, T. (2009). The extreme cold anomaly over southeast Asia in February 2008: Roles of ISO and ENSO. *Journal of Climate*, *22*(13), 3786–3801. https://doi.org/10.1175/2009JCLI2864.1

Hsu, P.-C., Qian, Y., Liu, Y., Murakami, H., & Gao, Y. (2020). Role of abnormally enhanced MJO over the Western Pacific in the formation and subseasonal predictability of the record-breaking Northeast Asian Heatwave in the Summer of 2018. *Journal of Climate*, *33*(8), 3333–3349. https://doi.org/10.1175/JCLI-D-19-0337.1

Huang, B., Thorne, P. W., Banzon, V. F., Boyer, T., Chepurin, G., Lawrimore, J. H., et al. (2017). Extended reconstructed sea surface temperature, version 5 (ERSSTv5): Upgrades, validations, and intercomparisons. *Journal of Climate*, *30*(20), 8179–8205. https://doi.org/10.1175/jcli-d-16-0836.1

Kanamitsu, M., Ebisuzaki, W., Woollen, J., Yang, S.-K., Hnilo, J. J., Fiorino, M., et al. (2002). NCEP–DOE AMIP-II reanalysis (R-2). *Bulletin of the American Meteorological Society*, *83*(11), 1631–1644. https://doi.org/10.1175/BAMS-83-11-1631

Klein, S. A., Soden, B. J., & Lau, N. C. (1999). Remote sea surface temperature variations during ENSO: Evidence for a tropical atmospheric bridge. *Journal of Climate*, *12*(4), 917–932. https://doi.org/10.1175/1520-0442(1999)012<0917:RSSTVD>2.0.CO;2

Lau, K. M., & Peng, L. (1987). Origin of low-frequency (intraseasonal) oscillations in the tropical atmosphere. Part I: Basic theory. *Journal of the Atmospheric Sciences*, *44*(6), 950–972.

Lee, J.-Y., Wang, B., Wheeler, M. C., Fu, X., Waliser, D. E., & Kang, I.-S. (2013). Real-time multivariate indices for the boreal summer intraseasonal oscillation over the Asian summer monsoon region. *Climate Dynamics*, *40*(1–2), 493–509. https://doi.org/10.1007/s00382-012-1544-4

Li, T., Wang, B., Chang, C.-P., & Zhang, Y. (2003). A theory for the Indian Ocean dipole-zonal mode. *Journal of the Atmospheric Sciences*, *60*, 2119–2135.

Lu, W., & Hsu, P.-C. (2017). Factors controlling the seasonality of the Madden-Julian Oscillation. *Dynamics of Atmospheres and Oceans*, *78*, 106–120. https://doi.org/10.1016/j.dynatmoce.2017.04.002

Madden, R. A., & Julian, P. R. (1971). Detection of a 40–50 day oscillation in the zonal wind in the tropical Pacific. *Journal of the Atmospheric Sciences*, *28*, 702–708.

Majda, A. J., & Stechmann, S. N. (2009). The skeleton of tropical intraseasonal oscillations. *Proceedings of the National Academy of Sciences of the United States of America*, *106*, 8417–8422. https://doi.org/10.1073/pnas.0903367106

Maloney, E. D. (2009). The moist static energy budget of a composite tropical intraseasonal oscillation in a climate model. *Journal of Climate*, *22*(3), 711–729. https://doi.org/10.1175/2008JCLI2542.1

Min, S.-K., Zhang, X., Zwiers, F. W., & Hegerl, G. C. (2011). Human contribution to more-intense precipitation extremes. *Nature*, *470*(7334), 378–381. https://doi.org/10.1038/nature09763

Ninomiya, K., & Shibagaki, Y. (2007). Multi-scale features of the Meiyu-Baiu front and associated precipitation systems. *Journal of the Meteorological Society of Japan*, *85B*, 103–122.
Roxy, M. K., Dasgupta, P., McPhaden, M. J., Suematsu, T., Zhang, C., & Kim, D. (2019). Twofold expansion of the Indo-Pacific warm pool warps the MJO life cycle. *Nature*, *575*(7784), 647–651. https://doi.org/10.1038/s41586-019-1764-4
Sampe, T., & Xie, S.-P. (2010). Large-scale dynamics of the Meiyu-Baiu rainband: Environmental forcing by the westerly jet. *Journal of Climate*, *23*(1), 113–134. https://doi.org/10.1175/2009JCLI3128.1
Sobel, A., Wang, S., & Kim, D. (2014). Moist static energy budget of the MJO during DYNAMO. *Journal of the Atmospheric Sciences*, *71*(11), 4276–4291. https://doi.org/10.1175/JAS-D-14-0052.1
Stuecker, M. F., Jin, F.-F., Timmermann, A., & McGregor, S. (2015). Combination mode dynamics of the anomalous northwest Pacific anticyclone. *Journal of Climate*, *28*(3), 1093–1111. https://doi.org/10.1175/JCLI-D-14-00225.1
Stuecker, M. F., Timmermann, A., Jin, F.-F., McGregor, S., & Ren, H.-L. (2013). A combination mode of the annual cycle and the El Niño/Southern Oscillation. *Nature Geoscience*, *6*(7), 540–544. https://doi.org/10.1038/ngeo1826
Tao, S., & Chen, L. (1987). A review of recent research on the East Asian summer monsoon. In C.-P. Chang & T. N. Krishnamurti (Eds.), *Monsoon meteorology* (pp. 60–92). New York, NY: Oxford University Press.
Wang, B., & Lin, H. (2002). Rainy season of the Asian–Pacific summer monsoon. *Journal of Climate*, *15*, 386–398.
Wang, B., Liu, F., & Chen, G. (2016). A trio-interaction theory for Madden–Julian Oscillation. *Geoscience Letters*, *3*, 34. https://doi.org/10.1186/s40562-016-0066-z
Wang, B., Wu, R., & Fu, X. (2000). Pacific–East Asian teleconnection: How does ENSO affect east Asian climate? *Journal of Climate*, *13*, 1517–1536.
Wang, L., Li, T., & Nasuno, T. (2018). Impact of Rossby and Kelvin wave components on MJO eastward propagation. *Journal of Climate*, *31*, 6913–6931.
Wheeler, M. C., & Hendon, H. H. (2004). An all-season real-time multivariate MJO Index: Development of an index for monitoring and prediction. *Monthly Weather Review*, *132*(8), 1917–1932. https://doi.org/10.1175/1520-0493(2004)132<1917:AARMMI>2.0.CO;2
Xie, P., & Arkin, P. A. (1997). Global precipitation: A 17-year monthly analysis based on gauge observations, satellite estimates, and numerical model outputs. *Bulletin of the American Meteorological Society*, *78*(11), 20.
Xie, P., Chen, M., Yang, S., Yatagai, A., Hayasaka, T., Fukushima, Y., & Liu, C. (2007). A gauge-based analysis of daily precipitation over East Asia. *Journal of Hydrometeorology*, *8*(3), 607–626. https://doi.org/10.1175/JHM583.1
Xie, S.-P., Kosaka, Y., Du, Y., Hu, K., Chowdary, J. S., & Huang, G. (2016). Indo-western Pacific Ocean capacitor and coherent climate anomalies in post-ENSO summer: A review. *Advances in Atmospheric Sciences*, *33*, 411–432.
Yang, D., & Ingersoll, A. P. (2013). Triggered convection, gravity waves, and the MJO: A shallow-water model. *Journal of the Atmospheric Sciences*, *70*(8), 2476–2486. https://doi.org/10.1175/JAS-D-12-0255.1
Yang, J., Liu, Q., Xie, S.-P., Liu, Z., & Wu, L. (2007). Impact of the Indian Ocean SST basin mode on the Asian summer monsoon. *Geophysical Research Letters*, *34*, L02708. https://doi.org/10.1029/2006GL028571
Zhang, C. (2005). Madden-Julian Oscillation. *Reviews of Geophysics*, *43*(2), RG2003. https://doi.org/10.1029/2004RG000158
Zhang, C., & Dong, M. (2004). Seasonality in the Madden–Julian Oscillation. *Journal of Climate*, *17*, 12.
Zhang, L., Wang, B., & Zeng, Q. (2009). Impact of the Madden–Julian Oscillation on summer rainfall in southeast China. *Journal of Climate*, *22*(2), 201–216. https://doi.org/10.1175/2008JCLI1959.1
Zhang, R., Sumi, A., & Kimoto, M. (1999). A diagnostic study of the impact of El Niño on the precipitation in China. *Advances in Atmospheric Sciences*, *16*, 229–241.
Zhang, W., Jin, F.-F., Stuecker, M. F., Wittenberg, A. T., Timmermann, A., Ren, H.-L., et al. (2016). Unraveling El Niño's impact on the East Asian Monsoon and Yangtze River summer flooding. *Geophysical Research Letters*, *43*, 11375–11382. https://doi.org/10.1002/2016GL071190
Zhang, W., Li, H., Jin, F.-F., Stuecker, M. F., Turner, A. G., & Klingaman, N. P. (2015). The annual-cycle modulation of meridional asymmetry in ENSO's atmospheric response and its dependence on ENSO zonal structure. *Journal of Climate*, *28*, 5795–5812.
Zhao, C., Li, T., & Zhou, T. (2013). Precursor signals and processes associated with MJO initiation over the tropical Indian Ocean. *Journal of Climate*, *26*(1), 291–307. https://doi.org/10.1175/JCLI-D-12-00113.1
Zhao, P., Yang, S., & Yu, R. (2010). Long-term changes in rainfall over eastern China and large-scale atmospheric circulation associated with recent global warming. *Journal of Climate*, *23*(6), 1544–1562. https://doi.org/10.1175/2009JCLI2660.1